

www.acsami.org Research Article

Plant Membrane-On-A-Chip: A Platform for Studying Plant Membrane Proteins and Lipids

Martin Stuebler, Zachary A. Manzer, Han-Yuan Liu, Julia Miller, Annett Richter, Srinivasan Krishnan, Ekaterina Selivanovitch, Barituziga Banuna, Georg Jander, Erik Reimhult, Warren R. Zipfel, Adrienne H. K. Roeder, Miguel A. Piñeros, and Susan Daniel*



Cite This: ACS Appl. Mater. Interfaces 2024, 16, 20092-20104



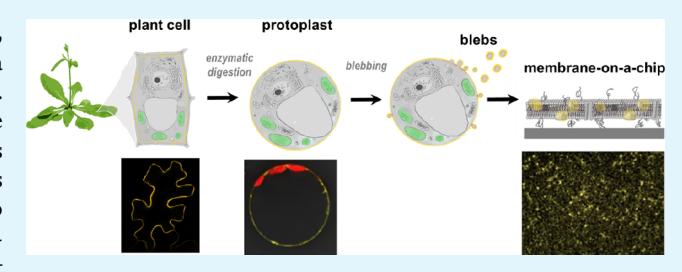
ACCESS

III Metrics & More

Article Recommendations

supporting Information

ABSTRACT: The cell plasma membrane is a two-dimensional, fluid mosaic material composed of lipids and proteins that create a semipermeable barrier defining the cell from its environment. Compared with soluble proteins, the methodologies for the structural and functional characterization of membrane proteins are challenging. An emerging tool for studies of membrane proteins in mammalian systems is a "plasma membrane on a chip," also known as a supported lipid bilayer. Here, we create the "plantmembrane-on-a-chip," a supported bilayer made from the plant



plasma membranes of Arabidopsis thaliana, Nicotiana benthamiana, or Zea mays. Membrane vesicles from protoplasts containing transgenic membrane proteins and their native lipids were incorporated into supported membranes in a defined orientation. Membrane vesicles fuse and orient systematically, where the cytoplasmic side of the membrane proteins faces the chip surface and constituents maintain mobility within the membrane plane. We use plant-membrane-on-a-chip to perform fluorescent imaging to examine protein—protein interactions and determine the protein subunit stoichiometry of FLOTILLINs. We report here that like the mammalian FLOTILLINs, FLOTILLINs expressed in Arabidopsis form a tetrameric complex in the plasma membrane. This plant-membrane-on-a-chip approach opens avenues to studies of membrane properties of plants, transport phenomena, biophysical processes, and protein—protein and protein—lipid interactions in a convenient, cell-free platform.

KEYWORDS: protoplast, plant cell membrane, supported lipid bilayer, bioelectronics, plant membrane

INTRODUCTION

The cell's interior is separated from its environment by a membrane, a fluid mosaic material that creates a semipermeable selective barrier. Cellular membranes are complex biomaterials composed of phospholipid bilayers with embedded and associated proteins arranged in dynamic, nonhomogeneous nanodomains, resulting in these multifaceted and diverse functions. In plant cells, the plasma membrane (PM) is in contact with the cell wall on the exterior and the cell's cytoskeleton on the interior, both of which can influence the localization, mobility, and function of the proteins within the membrane. These structures pose a big challenge for surfacebased characterization techniques aimed at studying and analyzing the cell membrane and the biochemical and biophysical processes that occur within it. Thus, biophysical studies of plant membranes, proteins, and lipids lag behind those of their mammalian counterparts.

A variety of *in vitro* approaches have been used to study the fundamental properties of biological membranes in a simplified and controlled microenvironment.² An established and robust system for studying mammalian plasma membrane phenomena is supported lipid bilayers, formed as a contiguous single sheet membrane bilayer supported on a solid surface, such as a glass

microscope slide.³ In recent years, alternative strategies have evolved to create supported hybrid membranes, in which the membrane is partially derived from the PM of mammalian cells.^{4–7} These hybrid-supported lipid bilayers are better mimics for the PM, as they directly incorporate native lipids and proteins from the PM into proteoliposomes through membrane blebbing and are subsequently used to create the supported bilayer. These hybrid bilayers are a good compromise between the complexity of a live cell and the simplistic reconstituted lipid systems for many applications. Over the past several decades, supported lipid bilayers have provided much insight into mammalian membrane biophysics, fundamental membrane processes, and membrane protein functions.^{8,9}

Turning to plants, a recent paper highlights open questions in deciphering the role of plant PM lipids in the immune response

Received: December 17, 2023 Revised: February 18, 2024 Accepted: February 21, 2024 Published: April 9, 2024





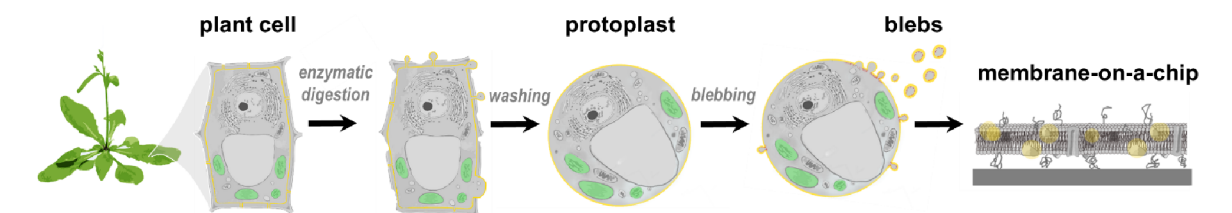


Figure 1. Process of building a plant membrane-on-a-chip from membrane vesicles derived from plant cell protoplasts. Here, *Arabidopsis thaliana* cells are released from their cell wall by enzymatic digestion, freeing the protoplast. Small vesicles, called "blebs," are released from the plasma membrane of the protoplast by chemical induction. These vesicles are then self-assembled into supported planar membranes on glass surfaces for biophysical and microscopy studies of the membrane proteins and lipids.

to invasion by pathogens and the challenges therein due to the lack of complexity in model systems. 10 Such studies could benefit from the biophysical approaches that have benefitted mammalian systems. Another recent review paper¹¹ promotes the application of biophysical approaches to plant membrane studies, but notes that while traditional biological techniques are suitable for studying complex systems, they are not easily leveraged for obtaining molecular-level understanding in plants. On the other hand, "bottom-up" model systems that currently exist for plants are too simplistic to capture more extensive or more complex system behavior, yet their easily controlled chemical composition is an asset for deciphering molecular level interactions. As such, it is apparent that a technology that meets in the middle between living plant tissues and cells and simplistic, reconstituted model membrane systems would bridge these worlds and fill a critical need.

In this paper, we adapt the supported lipid bilayer approach that has benefitted mammalian membrane biophysics to plant cells. We collected samples of the protoplast PM in the form of blebs and self-assembled them into a planar geometry on a flat glass microscope slide (Figure 1). This supported membrane contains the materials of the bleb, which include transgenic transmembrane proteins expressed in the protoplast PM, without the need for purification or detergent reconstitution of the proteins. In this planar format, the plant "membrane on a chip" is amenable to many surface analysis techniques and advanced microscopy tools that have benefitted mammalian cell studies, and we demonstrate a few of them here in this system. We show that this platform is amenable to several plant species and, thus a general approach suitable for studying both transmembrane and membrane-associated proteins, which can readily be incorporated from protoplasts into the supported lipid bilayer. As such, this advance opens the possibility for the plant community to benefit from this technology for analogous biophysical and biochemical studies of plant membranes.

RESULTS

Plant Membrane Protein Expression. To test if supported lipid bilayers were a suitable system to characterize plant intrinsic membrane proteins, we first examined different fluorescent fusion proteins expressed in three different plant species: *Arabidopsis thaliana* (dicot), *Nicotiana benthamiana* (dicot), and *Zea mays* (monocot). In *A. thaliana*, we expressed the *Arabidopsis* Rare Cold Inducible 2A (RCI2A) protein tagged with mCitrine; in *N. benthamiana*, we heterologously expressed the *Arabidopsis* Plasma membrane Intrinsic Protein 2A (PIP2;1) tagged with mCherry, and in *Z. mays*, we expressed the maize PIN1a (an auxin transporter) tagged with YFP (Figure 2A—C).

These proteins have disparate functions in plants. RCI2A is expressed in response to low temperature, dehydration, salt

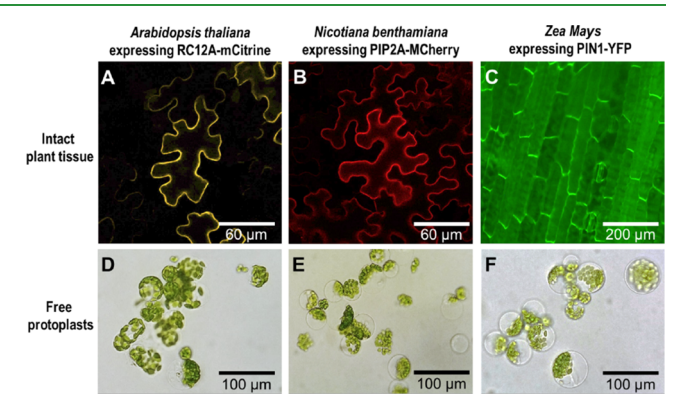


Figure 2. Micrographs of protein expression within intact leaf tissue and released protoplast from these cells. (A–C) Confocal images of plant cells expressing fluorescently tagged membrane proteins within intact tissue: mCitrine-RCI2A in *A. thaliana* (A), PIP2;1-mCherry in *N. benthamiana* (B), and PIN1a-YFP in *Z. mays* (C). (D–F) Bright-field images of the corresponding released protoplasts, free of the cell wall. Protoplasts assume a spherical shape bounded by a plasma membrane surrounding a clear intact vacuole and green chloroplasts.

stress, and abscisic acid and is critical to driving compositional changes in the plasma membrane necessary for the plant's adaptive response to cold adaptation. PIP2;1 is an aquaporin that facilitates water transport across plasma membranes and has been recently shown to be gated by protons and divalent cations as regulators of water flux, signal transduction, and nutrient uptake through them. Both RCI2A and PIP2 fluorescent fusion proteins are often used as PM markers when expressed under ubiquitous promoters. PIN1 is a plant hormone transporter critical for the efflux of auxin across the plasma membrane necessary for plant development and growth. The expression of all three fluorescent fusion proteins is abundant and confined to the membranes (Figure 2A—C).

Protoplast Release from Cell Wall and Formation of Bleb Vesicles. The plant cell wall was removed to gain access to the intrinsic proteins expressed at the PM. For this purpose, we isolated protoplasts following standard protocols (see Methods). The intact protoplasts assumed spherical shapes with visible intact organelles inside, confirming their structural integrity (Figure 2D–F). We adapted a protocol used to generate blebs from mammalian cells and subjected the protoplasts to a chemical blebbing process that induces the shedding of "blebs" (vesicles) from the cell PM. ^{6,7,17} These blebs are small-scale "biopsies" of the plant PM and contain the membrane proteins and local membrane components in the native membrane vesicle.

These blebs are the raw material later used to self-assemble planar, supported membranes on glass microscope slides, thereby creating a protoplast "membrane-on-a-chip." Blebbed vesicles across all plant species are on the order of several hundred nanometers in diameter and only slightly negatively charged in buffer (Figure S1). Bleb sizes in the submicron range and low surface charge are parameters that are important for the design and reproducibility of the supported membrane self-assembly.

Formation of Supported Membranes from Bleb Vesicles and Fusogenic Liposomes. To create self-assembled supported membranes out of plant protoplast blebs, we adapted a process successfully used with blebs from mammalian cells^{6,7} or outer membrane vesicles from bacteria¹⁸ (Figure 3, left-hand side). To visualize the formation process,

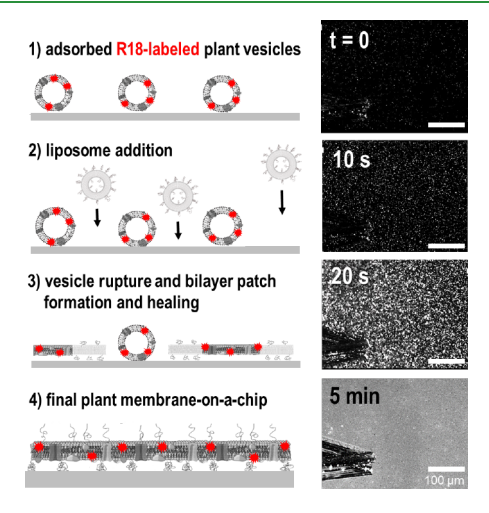


Figure 3. Scheme of plant protoplast planar bilayer formation and monitoring of formation via fluorescence microscopy. (Left hand side, 1-4) Illustration of the self-assembly process of forming a planar membrane from plant protoplast vesicles via the addition of fusogenic liposomes. The red stars represent the intercalating membrane fluorophores (R18) associated only with the plant vesicles. (Right hand side) Time-lapse images monitoring bilayer formation over 300 s of bleb vesicles from N. benthamiana. The fusogenic liposomes are not labeled. Thus, the spreading of the fluorescence signature observed in the images is indicative of plant vesicle rupture and planar membrane formation. The black scratched area (marked by an arrow) is intentionally made with a dissection tool to ensure that the focal plane remains at a constant z-position throughout the formation process. After 5 min, the plant membrane material has intermixed with the liposome material, forming a uniform planar membrane. Scale bar: $100 \mu m$.

the plant-derived bleb vesicles were labeled with membraneintercalating fluorophore Octadecyl Rhodamine B chloride (R18). These membrane-labeled vesicles were then adsorbed to the glass surface and observed as fluorescent puncta (Figure 3, right-hand side). Next, pure liposomes (unlabeled) that readily rupture to form planar bilayer patches on the glass surfaces were added. When these liposomes rupture next to the adsorbed bleb vesicles, they induce their rupture. Fusogenic liposomes were formulated as 1-palmitoyl-2-oleoyl-sn-glycero-3-phosphocholine (POPC) mixed with 0.5 mol % of polyethylene glycol conjugated lipid (1,2-dioleoyl-sn-glycero-3-phosphoethanolamine-N-[methoxy(polyethylene glycol)-5000]). The inclusion of polyethylene glycol conjugated lipids in the supported membrane provides a spacer between the glass surface and the proximal membrane leaflet (Figure 3). 19 This space is important for maintaining protein mobility in the membrane plane (discussed below) as mobility is a key parameter for some biophysical and biochemical processes in the membrane. The rupturing, the formation of planar bilayer patches, and the healing together of the patch edges as the process proceeds are evident by the increasingly homogeneous distribution of the fluorophores originally trapped in the plant vesicle membranes (Supplemental Video 1). The process results in a uniform planar membrane film supported by the glass surface after about 5 min (Figure 3, right-hand side). We note that adding these fusogenic liposomes changes the composition of the membrane formed by diluting with phospholipids; however, further testing (see below) revealed that the membrane maintains many features similar to plant plasma membranes, including membrane protein mobility.

Supported Membranes are Contiguous and Maintain the Mobility of Constituents. A salient feature of cell membranes is the lateral mobility of their constituents. Here, we characterized the lipid mobility of the newly formed planar protoplast membrane as a measure of supported membrane quality: that is, being free of unruptured vesicles, disconnected patches, or holes that would otherwise disrupt the diffusion of constituents in the supported bilayer. We used the fluorescent R18 label dispersed throughout the self-assembled membrane to assess the 2D lateral mobility of the probe in the membrane.

To obtain the diffusion coefficient, we photobleached an \sim 20 μ m diameter circle with a laser beam and then monitored the fluorescence recovery in this spot over time (Figure 4A). If the membrane is planar and the lipids are mobile laterally within that

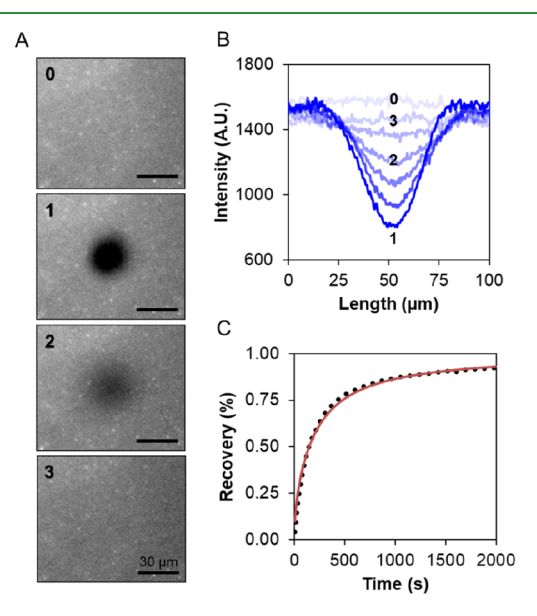


Figure 4. Fluorescence recovery after photobleaching (FRAP) of *N. benthamiana* demonstrates the formation of high-quality supported lipid bilayers. (A) Images of a photobleached supported membrane made from *N. benthamiana* blebs. 0 shows an image of the prebleach fluorescence of the region, 1 (t=0 s) imaged immediately following bleaching, and 2 (t=100 s) and 3 (t=2036 s) are imaged during the recovery time. (B) Profiles of the intensity were drawn across the images. (C) Fluorescence recovery as a function of time (black circles). The data were fitted to the 2D diffusion equation (red line); the goodness of the fit indicates that a planar membrane has been formed. Data for the other plant species are presented in Supplemental Figure S2. The diffusion coefficient (D) and mobile percentage (MF) for the three different plant species were derived as discussed in Materials and Methods and are presented in Table 1.

plane, then the fluorescence recovery will follow a simple 2D diffusion curve because lipid exchange is only possible from the perimeter of the bleached region (Figure 4B). The experimental fluorescence recovery data followed an ideal 2D diffusion model, indicating that a planar membrane was formed (Figure 4C).

The percent mobility is a measure of the lipids that are mobile in the photobleached region. The vesicles are on the order of several hundred nanometers, while the photobleached area is on the order of tens of microns. Thus, unruptured plant vesicles or disconnected patches that are not healed into the planar membrane film will be unable to recover their fluorescence after bleaching, reducing the absolute fluorescence value that is recovered in the bleached area. The percent mobility of the supported bilayer derived from N. benthamiana was ~95%, indicating that it was a high-quality supported membrane, free of defects that would prevent full recovery (Figure 4C). The A. thaliana and Z. mays bilayers also had high percent mobility, confirming high-quality supported membranes (Supplemental Figure S2). These results indicate that planar membranes derived from each vesicle type are contiguous over micrometerscale dimensions, even though the diffusion coefficients vary (Table 1). Variation in diffusion coefficient is expected for vesicles from different plant species that have different membrane chemistries and components.²⁰

Table 1. Lipid Diffusion and Mobility Characteristics in the Supported Bilayer

plant species	A. thaliana	N. benthamiana	Z. mays
diffusion coefficient ($\mu m^2/s$)	0.48 ± 0.14	0.15 ± 0.16	0.35 ± 0.15
mobile percent (%)	95 ± 2.1	94 ± 2.2	95 ± 2.8

Transmembrane Proteins are Oriented with their Cytosolic Face Adjacent to the Slide. Recapitulation of the native protein orientation in the supported membrane is crucial to the proper biological function and activity of the protein in further assays. We followed an established protocol to determine protein orientation in supported membranes.^{6,7,17} For this purpose, we took advantage of two protease cleavable sites between the mCitrine and the rest of the protein in the mCitrine-RCI2A chimera²¹ (see Supplemental Figure S3 for the sequence). In A. thaliana leaf cells, mCitrine-RCI2A localizes to the plasma membrane and expression is confirmed by the presence of fluorescence there (Figure 5A–C). The predicted orientation of the mCitrine-RCI2A protein in planta is with the N-terminal mCitrine on the cytoplasmic side of the membrane, followed by one transmembrane domain, a short extracellular loop, and a second transmembrane domain with the C terminus facing the cytoplasm (Figure 5D).

To conduct the orientation assay, we first created a supported membrane with blebs from *A. thaliana* protoplasts expressing mCitrine-RCI2A. Protein expression in the supported membrane was observed by using total internal reflection fluorescence microscopy (TIRFM). TIRFM is a convenient microscopy technique because only a region within a few hundred nanometers from the glass-buffer interface is illuminated. Therefore, only fluorescently labeled proteins within the supported membrane contribute to the fluorescence image. We considered that the plant vesicles could rupture in several ways, resulting in proteins having the same orientation as *in planta* (with the extracellular side facing toward the buffer), with the proteins facing the opposite direction, or some mixture

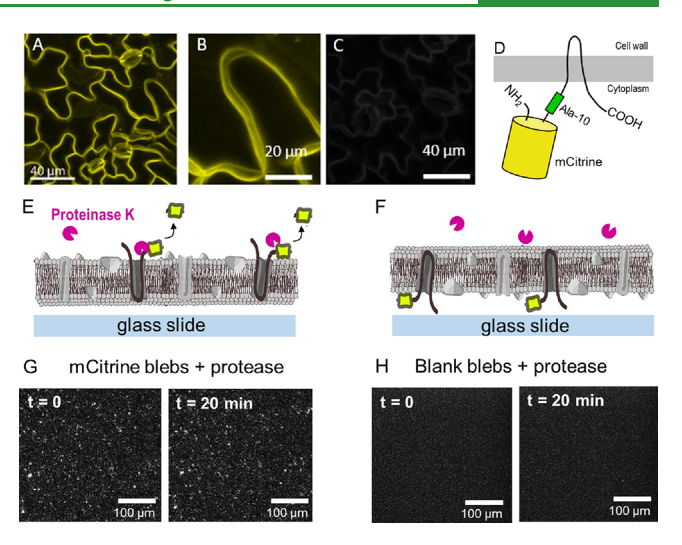


Figure 5. Cytosolic side of the supported bilayer faces the glass slide. (A) Yellow fluorescence signal in intact plant cells from A. thaliana expressing mCitrine-RCI2A. (B) Magnified view of (A). (C) Nonexpressing, wild type plant membrane control (no expression of mCitrine-RCI2A) does not show any autofluorescence. (D) Diagram of the native protein orientation of mCitrine-RCI2A in the protoplast. (E) and (F) are possible orientations of the proteins and have cleavage site access. In (E), the cleavage site is exposed when proteins are oriented with the cytoplasmic domains toward the buffer containing the protein, and the protease (purple) can cleave off the fluorophore. In (F), the proteins are oriented with the extracellular domains toward the buffer, and the cleavage site is inaccessible to the protease. (G) Images before (t = 0; 129 particles) and after (t = 20 min; 135 particles) protease exposure of the supported plant membrane expressing mCitrine-RCI2A. (H) Nonexpressing, wild type plant membrane (blank), same as in (C), before and after protease exposure, shows there is no background fluorescence from other membrane components or the protease during this assay.

of both (Figure 5E,F). We determined the orientation by assessing the fluorescence level after protease exposure. If the mCitrine label were facing upward toward the buffer (the protein upside-down relative to in planta), then mCitrine would be cleaved off during protease exposure and float out of the excitation field (Figure 5E). Alternatively, if the mCitrine label was inaccessible to the protease because it was oriented beneath the supported membrane, no significant fluorescence change would occur (Figure 5F). Before protease exposure, the mCitrine-RCI2A protein appeared as spots in the supported lipid bilayer (Figure 5G). After 20 min of protease exposure, the signal did not change, indicating the cleavage site was not accessible (Figure 5G, t = 20 min). It follows that the protein was oriented as in planta, with the outward-facing domains toward the buffer and the mCitrine toward the glass slide on the chip (Figure 5F). Therefore, the buffer side is equivalent to the extracellular space, and the glass side represents the cytoplasmic side. As a control, no background signal was observed in a supported membrane that had no mCitrine-RCI2A protein either before or after protease exposure (Figure 5H). As an additional control, we verified that the mCitrine-RCI2A protein is cleavable by first sonicating the vesicles to flip the membrane vesicle's orientation around, purposely ensuring some fraction of proteins will be oriented upside down where the cleavage site becomes accessible to proteases after planar membrane formation. In this set of experiments, we observe a loss of fluorescence signal due to enzymatic cleaving within 20 min (Supplemental Figure S4).

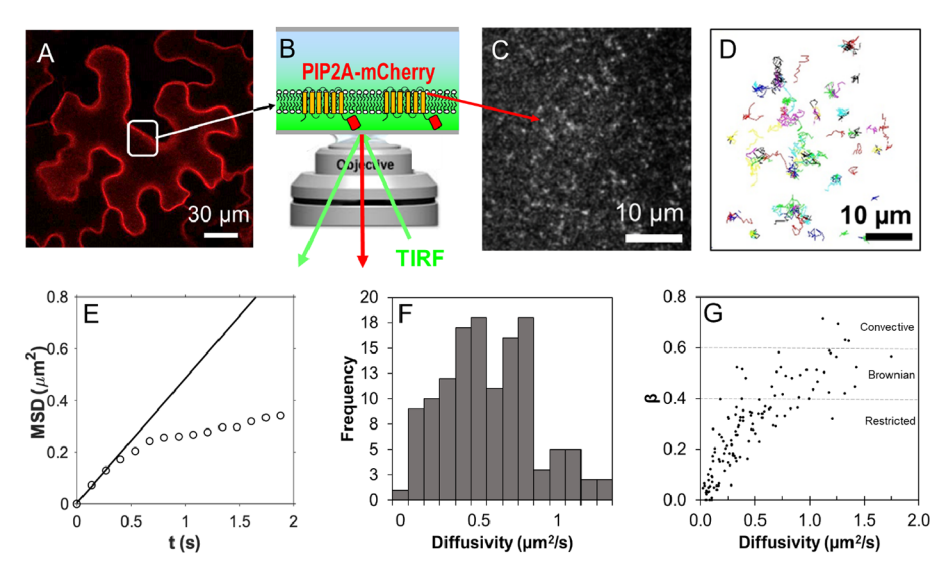


Figure 6. Single-protein tracking of PIP2;1-mCherry shows the lateral mobility in the supported N. benthamiana membranes. (A) PIP2;1-mCherry expressed in an intact plant cell, marking the plasma membrane. This image is adapted from Figure 2B. (B) Diagram of the TIRF microscopy set up with a supported membrane expressing the mCherry-tagged protein excited by the evanescent light field. (C) TIRFM snapshot: the bright spots are protein particles. (D) Mean square displacements (MSD) for individual proteins taken over several time steps (at least 20 frames). The path of each protein particle is tracked in a different color. (E) An example graph of the MSD versus time from one particle in (D). The tangent line of the first three points was used to determine the diffusion coefficient before confinement occurs. (F) Distribution of diffusion coefficients obtained from MSD plots like (E). (G) The β parameter, which gives a measure of confinement.

Table 2. Protein Diffusion and Mobility Characteristics in a Supported Bilayer

plant species	A. thaliana	N. benthamiana	Z. mays	A. thaliana
protein	mCitrine-RCI2A	PIP2;1-mCherry	PIN1a-YFP	PIN1-GFP
diffusion coefficient $(\mu m^2/s)$	0.73 ± 0.35	0.63 ± 0.32	0.48 ± 0.13	0.50 ± 0.21
mobile percent (%)	85.1	72.7	57.3	84.2
confinement (%)	60.8	71.1	46.5	56.5

Single-Particle Tracking of Transmembrane Proteins Demonstrates their Lateral Mobility in the Membrane Plane. *In planta*, some transmembrane proteins can diffuse laterally within the membrane, which can be critical for their interactions with other proteins and function; therefore, as a measure of supported lipid bilayer function, we tested the diffusibility of proteins in the membrane. Diffusion can be modulated by lipid domains or by interactions with the cytoskeleton or the cell wall. In this platform, however, the cell wall and cytoskeleton are absent, but it is possible that there are lipid domains and some interaction with the support that can limit protein mobility.

To minimize interactions with the support, we included a small amount of pegylated lipid to provide some additional space to accommodate the cytosolic portion of the protein that would be facing toward the glass slide (as mentioned above). Pegylated lipids have an inert poly(ethylene glycol) polymer attached to the headgroup of the lipid. Pegylated lipids have previously been used in supported bilayer platforms of synthetic mixtures, where it has been shown that the pegylated lipids are themselves mobile. For our formulation, the approximate globular size of the polymer should be ~5 nm, ^{23,24} providing about 4 nm more space than the typical supported lipid bilayer on glass. This cushioning effect is apparent because, without the addition of these lipids, we observed little to no protein mobility, presumably because the cytosolic portions that extend beyond 1 nm stick to the glass support. ^{6,25}

To form the bilayers examined here, we adsorbed blebs from *N. benthamiana* expressing PIP2;1-mCherry and ruptured them

with a nonfluorescent pegylated liposome formulation. In Supplemental Video 2, the rupture, bilayer formation, and subsequent protein diffusion in 2D are readily apparent. Initially, the adsorbed blebs are immobile punctate spots. These puncta are visible due to the fluorophore-tagged protein that is expressed in the blebs. When the fusogenic liposomes rupture on the glass, they induce the rupture of the neighboring blebs and the healing of the newly formed bilayer patches to create a contiguous bilayer. After this bilayer is created, the fluorescent puncta begin to move in a random fashion around the site of the initial adsorption, presumably because they are now free to diffuse within the bilayer plane.

We characterized the mobility of the overexpressed transmembrane proteins in the supported protoplast membranes. Supplemental Video 3 shows a fully formed bilayer with PIP2;1mCherry diffusing and colored trajectories of the protein pathways superimposed on the images with each time step. Since all of the proteins used here have fluorescent tags, we used single-particle tracking techniques to obtain the mean square displacements (MSD) as a function of time to acquire both the homogeneous "local" diffusion coefficient and classify the protein confinement over long times after sampling a wider membrane area. Using TIRFM on PIP2;1-mCherry in supported membranes made from N. benthamiana, we tracked the movement of approximately 150 individual fluorescent particles over time (Figure 6A-D). The tracks of the single particles were plotted with time, and the tangent of the slope over the first three-time steps (interval ~130 ms) was used to obtain the diffusion coefficient in the local membrane milieu

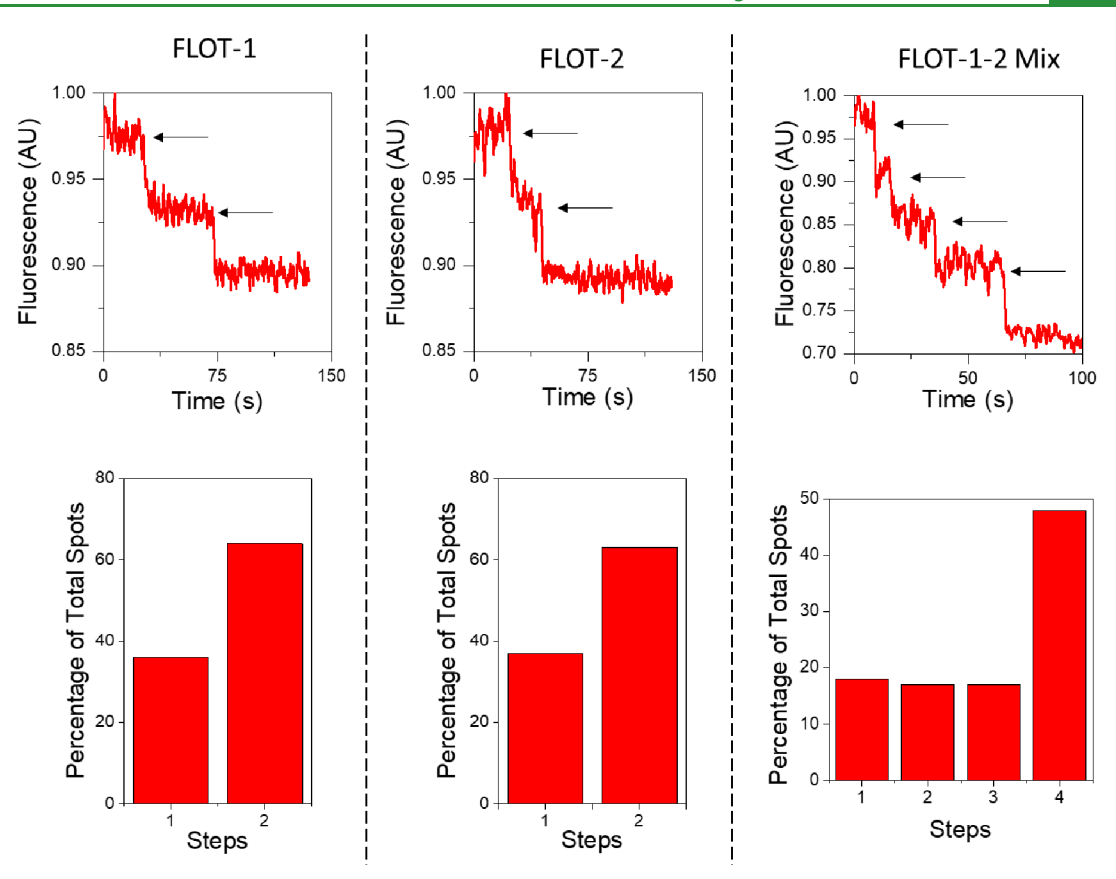


Figure 7. Subunit photobleaching experiment for the *A. thaliana* AtFLOT1 AtFLOT2 or 1:1 mix of the two FLOTILLINs GFP chimeras. Top row: Representative intensity—time trace of the photobleaching steps observed for the individual or mixed FLOTILLINs. The data are presented without subtracting the background fluorescence. Single photobleaching events in the example traces shown in each graph are indicated by horizontal arrows. Bottom row: percentage of the number of photobleaching steps recorded in a spot from the intensity—time traces (n = 217, 174, and 121 individual spots were measured for FLOT1, FLOT2, and FLOT1–2-mix, respectively). Individual measurements were obtained from at least five different membrane patches and repeated on three independent plant transformations and protoplast preparations.

(Figure 6E). The initial diffusion coefficients of the PIP2;1-mcherry proteins tracked in this sample were distributed from 0.1 to 1.3 μ m²/s (Figure 6F and Table 2). At shorter time scales, the MSDs were within the "Brownian" regime, which is characteristic of a protein sampling its immediate lipid environment that is presumably relatively homogeneous (Figure 6E,G). ^{6,26,27}

At longer times, the increase in MSD values with time tapers off, characteristic of the restriction of a protein's motion as it samples more of its wider surrounding (heterogeneous) membrane environment. If the wider membrane environment were homogeneous and the same as the immediate surrounding environment, the data trend would remain a straight line with the first three points, with a slope of twice the diffusion coefficient (a constant value). In the case in which the protein sees a more heterogeneous environment as it samples a larger area, the slope changes as time proceeds (as does the diffusion coefficient), which is what we observe in most of the tracks here, indicating that the planar membranes likely have heterogeneity in composition or domains.

Over long times, when the protein has had more time to explore a more extensive area, we measured an additional parameter, β , from the moment scaling spectrum (MSS) analysis. The moments of displacement are first determined for each protein. Then, the slope of moment scaling factor versus moment order is β . This slope, β , reports the particular protein's diffusion mode in this larger membrane region. β

values between 0.4 and 0.6 are typically considered Brownian (unhindered) diffusion, where the protein undergoes a random walk as it diffuses (and the MSD plot stays linear with a constant slope). β values greater than 0.6 are considered active transport (convective motion), where the protein is purposely biased in its diffusive motion, usually by a gradient or external force; and β values less than 0.4 are considered restricted diffusion, or diffusion that is confined in some way, perhaps by physical barriers or compositional variations in the membrane. ^{6,28,29} We find that about 70% of PIP2;1-mCherry particles in this platform show some confinement behavior, and nearly all of the rest show Brownian motion (Figure 6G). It is plausible that the confined behavior is derived from the proteins that reside within a more "native-like" membrane domain, while those exhibiting Brownian motion may be diffusing in the regions that are dominated by the lipids derived from the fusogenic liposomes.

We carried out similar analyses for the mCitrine-RCI2A in *A. thaliana*, and PIN1a-YFP in *Z. mays* supported membranes (Supplemental Figure S5 and Table 2). The average diffusion coefficients we detected in the supported lipid bilayer were one to two orders of magnitude higher than the diffusion coefficients of these proteins reported *in planta* ($\sim 10^{-1} \ \mu m^2/s$ in the supported lipid bilayer rather than $\sim 10^{-2}$ or $\sim 10^{-3} \ \mu m^2/s$ *in planta*). $^{30-32}$ In planta, interactions of transmembrane proteins with the cell wall and cytoskeleton limit diffusion, 1,30,31 so it is not surprising that the diffusion rates in the supported lipid bilayer platform would exceed those *in planta*, especially because

we purposefully added a cushion to limit the protein interaction with the glass support. Thus, the in vitro environment of the supported lipid bilayer platform enables the analysis of diffusibility relative to membrane composition and microdomains without these other influences; it also allows a comparative analysis based on protein size. Overall, we observe that the relative order of the diffusion coefficient is RCI2A > PIP2;1 > PIN1a (Table 2). RCI2A (also known as LTi6a, AT3G05880) is a two-pass transmembrane protein, which consistently exhibits higher diffusibility than PIP2;1 in vivo and is known as a fast diffusible membrane protein. 30,31 The PIP2;1 subunit has six membrane-spanning α -helices with the native functional transporter arranged as homo- or heterotetramers, and PIN1a has ten transmembrane passes and a large intracellular loop. Thus, the relative order we observed for the diffusion coefficient in this platform is aligned with protein size.33

We next compared two orthologous proteins, PIN1a-YFP from maize and PIN1-GFP from Arabidopsis, stably expressed in their respective plant species. Interestingly these proteins exhibited similar diffusion and mobility characteristics, except PIN1-GFP from Arabidopsis had a higher mobile fraction (Table 2). In studies of PIN2 (a paralog of PIN1) diffusion in the native plasma membrane confined by the cell wall, the mobile fraction is reported as $\sim 17\%$. This low percentage is attributed to the presence of the cell wall, which confines the protein to a specific region of the plasma membrane in planta to ensure the directional transport of auxin. In this work, we achieve a higher mobile fraction (\sim 57% for PIN1a-YFP in maize and \sim 82% for PIN1-GFP in Arabidopsis), presumably because this platform lacks the cell wall interaction and because the PEG cushion minimizes the interaction of the protein with the glass support, allowing an increased fraction of proteins to remain mobile.

FLOTILLIN1(FLOT1) and FLOTILLIN 2 (FLOT2) Form an Oligomeric Complex in the Plasma Membrane. An advantage of this planar platform is that it is compatible with fluorescence microscopy analysis methods. In this next set of experiments, we test whether membrane-associated proteins were also incorporated into the supported lipid bilayer via blebs from the protoplasts and determine the oligomeric state of those proteins. In planta, FLOTILLINs are localized to microdomains within the membrane and are involved in endocytosis as well as signaling.37-41 In A. thaliana, FLOTILLINs lack a transmembrane domain but are still membrane-associated. 37,42,43 In vivo, AtFLOT1 and AtFLOT2 are mainly immobile in the membrane, and the cell wall contributes to the lack of lateral mobility of the nanodomains. 42 We found that AtFLOT1 and 2-GFP transiently expressed in N. benthamiana were incorporated into the supported lipid bilayer, indicating that membraneassociated proteins can also be assayed with this platform. While it is well-established that mammalian FLOTILLINs form stable homotetramers and heterotetramers in membrane microdomains, 44 the oligomeric state of AtFLOT1 and 2 has not yet been evaluated.

We tested the multimeric nature of these proteins with our platform by single-molecule subunit counting using supported lipid bilayers containing GFP-tagged AtFLOT1 or 2. We first established the stoichiometry of AtFLOT1 or 2 independently by imaging the GFP-tagged FLOTILLINs under TIRF microscopy. The basic principle of single-molecule subunit counting relies on counting the discrete photobleaching steps of GFP tagged to the protein-of-interest. Thus, the number of photobleaching steps would be equal to the number of GFP-

tagged subunits in a single protein complex. Both GFP-tagged AtFLOT1 and AtFLOT2 photobleached as two discrete steps under TIRF conditions (Figure 7), indicating that AtFLOT1 and 2 oligomerize as dimers when imaged independently. To determine the oligomeric state of both FLOTILLINs, each bleb sample was mixed in 1:1 ratio before forming supported bilayers. We report that the mixed samples photobleached predominantly in four steps (Figure 7), indicating the formation of tetramers. Given the use of a single fluorescent label (GFP) in this study, we cannot discern the ratio of AtFLOT1 and AtFLOT2 in the tetrameric complex. However, these results demonstrate that, like the mammalian FLOTILLINs, the Arabidopsis ones form a tetrameric complex in the plasma membrane. The determination of the oligomeric state demonstrated here illustrates the potential application of this platform for investigating many types of protein-protein interactions and its potential application to a variety of other detailed molecular studies that will advance our understanding of plant proteins.

DISCUSSION

While this cell-free, in vitro supported lipid bilayer platform captures key properties of the plasma membrane, there are several aspects that do not faithfully replicate the cell's in planta state. First, the absence of the cell wall and the cytoskeleton relieves two major constraints found in planta that limit the diffusibility of some membrane proteins. 1,42,46 However, the absence of these structures in this platform allows one to focus exclusively on the protein-protein and protein-lipid interactions within the membrane. While that can be an advantage to this simplified system for some studies, it also results in the diffusion coefficients of transmembrane proteins in these systems being 10 to 100 times higher than those observed in planta. Second, the introduction of fusogenic liposomes affects the composition of the membrane. At this stage, it is difficult to quantify the exact percentage of lipids in the bilayer that come from the liposomes versus those from the protoplast membrane. However, it is possible to experimentally alter the lipid composition and the relative amounts surrounding the integral proteins, adding a level of experimental flexibility, as one could, for example, examine the effect of the lipid environment on a transporter functionality or oligomerization state. 47-49 Third, the space between the cover glass and the membrane impacts protein diffusion. Interactions between the cytoplasmic side of the protein and the glass slide can artificially anchor the protein, limiting diffusion; on the other hand, it may be advantageous to immobilize proteins for some applications. Depending on the application of the plant membrane on a chip, it is important to keep these three aspects in mind when interpreting results and extrapolating in vivo vs in vitro observations.

CONCLUSION

This cell-free platform is the first biomimetic supported bilayer of the plant plasma membrane made from native materials from plant protoplasts, including transgenic proteins in the plant PM. Importantly, there is no need to isolate these membrane proteins from the protoplast membrane, bypassing purification, and reconstitution steps. Such extraction techniques often use detergents to solubilize membrane proteins and risk disrupting protein function and the native lipid—protein association. This can have consequences, as many proteins are regulated by a complex cascade of protein—protein and lipid—protein interactions in various ways. 51,52 Using the blebbing protocol,

proteins in plant vesicles that bounded from the protoplast PM can be incorporated directly onto the chip with their associated lipid components; for transmembrane proteins that are notoriously hard to handle, these are significant advantages.

We demonstrate that three different plant transmembrane proteins (i.e., a water transporter, a hormone transporter, and a protein produced in the membrane in response to stress) and peripheral membrane proteins (FLOTILLINs) expressed in three different plant species could be successfully integrated into this platform, making it a general approach. Furthermore, we show that proteins in the resultant supported planar membranes are oriented as they are in planta, with the cytosolic side facing toward the glass surface and the extracellular side facing toward the buffer accessible to interact with any ligand, ion, or pathogen of interest. Diffusion behavior generally mirrors that observed in planta, including Brownian motion and confinement. One limitation of this platform is the lack of cellular traffic by the cellular machinery (e.g., microtubule, or actin networks), which our cell-free platform lacks. We also demonstrate this platform's usefulness in characterizing the oligomeric state of membranebound proteins. As a proof of concept, we showed that AtFLOT1-GFP and AtFLOT2-GFP independently associate as dimers in the membrane, but when AtFLOT1-GFP and AtFLOT2-GFP are both present in the membrane, they assemble predominantly as tetramers. Our result parallels the finding in mammalian cells that FLOTILLINs associate to form tetramers. 44 This experiment further demonstrates that this platform can be used to analyze the interactions of proteins that were initially expressed in different plants and were mixed in the formation of the supported lipid bilayer, enabling the possibility of unique experimental designs for future biophysical studies.

This cell-free approach opens up these biomembranes for many fundamental studies that would be difficult or impossible in planta or with live protoplasts in vitro. The main advantage of this platform is its compatibility with state-of-the-art microscopy and biophysical characterization tools, including surface plasmon resonance, quartz crystal microbalance, and atomic force microscopy, to name a few, that enables the application of these tools to the plant membrane biology field to answer outstanding questions. 10,11 This biomimetic platform opens up the possibility for many different kinds of future experiments, for example, extensions to the direct interaction between a pathogen and membrane proteins and lipids can be investigated. 11,53 Given recent advances by us and others in merging supported lipid bilayers with conducting polymer surfaces, 5 we anticipate that it will be possible to extend this approach to directly measure the electrogenic transport as ionic species are translocated across plant membranes, 56 which will open up new ways to conduct fundamental studies of transporter function in a convenient and controlled manner. As such, the platform we present here is a useful stepping stone toward being able to screen many mutants of a protein transporter and generate a functional profile that maps to those mutations.

METHODS

Plant Materials, Growth Conditions, and Protoplast Isolation. Three plant species expressing a variety of integral membrane proteins were used in this study:

Arabidopsis thaliana. The Rare Cold-Inducible 2a (RCI2A) Protein. pLH13 is a stably transformed line expressing 35S::mCitrine-RCI2A, a monomeric yellow fluorescent protein (mCitrine) and AtRCI2A fusion protein constitutively expressed under the control of the 35S promoter. pLH13 plants were grown in a Percival growth chamber at 22 °C with 24-h light regimen \sim 100 μ mol fluorescent light intensity. Protoplasts

expressing 35S::mCitrine-RCI2A were isolated from leaf mesophyll tissue from rosette leaves of 3-5 week-old plants. Leaf strips of 1 mm width were cut from 0.5 g of leaf tissue, excluding the midrib region and the petiole. The leaf tissue strips were vacuum infiltrated for 3 min until reaching 80 kPa in an enzyme solution consisting of 500 mM Mannitol, 20 mM MES, 5 mM CaCl₂, 2 mM 2-Mercaptoethanol, 25% v/v Cellulase R10 (Yakult Pharmaceutical), 5% v/v Maceroenzyme R10 (Yakult Pharmaceutical), and 0.001% Bovine Serum Albumin (BSA), pH 5.6. The air bubbles emerging at the plant material surface could be detached by gently bumping the vacuum chamber on the bench and was followed by slowly releasing the vacuum inside the chamber. The vacuum was once again established, repeating the latter process two to three times until the submerged material was of homogeneous dark color. At this point, the vacuum was kept constant at 80 kPa for 3 h at room temperature (23 °C). Released protoplasts were then pelleted by centrifugation at 250 rcf for 3 min and gently resuspended in 20 mL filtered GPMVM solution consisting of 500 mM Mannitol, 150 mM NaCl, 10 mM HEPES, 2 mM CaCl₂ at pH 5.6). Cells were washed twice in GPMVM, with the final pellet being resuspended in GPMVM at the desired cell density.

Arabidopsis thaliana PIN-FORMED1 Auxin Efflux Carrier (PIN1). We used a stably transformed line expressing a PIN1::GFP fusion protein expressed under the control of its native promoter.⁵⁷ Therefore, PIN1 is not expressed in leaves but in the root meristem and the vasculature. Seedlings were grown for 5 days on 1/2x MS plates (with 2% sucrose and 0.5 mg/mL MES pH 5.7) oriented vertically and overlain with a sterile cellophane disk. Protoplast isolation from PIN1-GFP *Arabidopsis* roots was performed as described by Birnbaum et al. with minor modifications. ⁵⁸ On day 5, the cellophane disk was used to remove seedlings from the plate, and roots were excised from the seedlings with a razor blade. Roots from about 20 plates were transferred into a 70 μ m cell strainer placed in a small Petri dish (60 \times 15 mm²) containing 10 mL of an enzyme solution consisting of 10 mM KCl, 2 mM MgCl₂, 2 mM CaCl₂, 1 mg/mL BSA, 0.39 mg/mL MES, 600 mM Mannitol, 15 mg/mL Cellulase R10 (PhytoTechnology C224), 1 mg/mL Pectolyase (Sigma), pH 5.5. The protoplasting roots were incubated at 26 °C on an orbital shaker at 100 rpm for 1 h and gently pressed against the strainer every 20 min. The cell strainer containing root debris was removed, and the protoplasting solution was again strained through a new 70 µm mesh cell strainer into a 50 mL tube. Released protoplasts were then pelleted by centrifuging at 500g at 4 °C for 6 mi, and gently resuspended in 10 mL of the protoplasting buffer without enzymes. Cells were washed twice with the final pellet being resuspended in the buffer at the desired cell density.

Nicotiana Benthamiana. Transiently transformed plants were created via Agrobacterium tumefaciens (strain GV3101) mediated transformation.

The Plasma Membrane Intrinsic Protein (The PIP2;1 Aquaporin). The expression of the PIP2;1:: mCherry chimera, in which the monomeric red fluorescent protein is C-terminally fused to PIP2;1, was driven by the constitutive AtUBQ10 promoter.

The Plasma Membrane-Associated Flotillins (FLOT1 and FLOT2). The expression of the Arabidopsis FLOT1 and FLOT2, GFP chimeras was driven by a 35S promoter. 42 Transiently expressing plants were generated using A. tumefaciens-mediated transformation. Briefly, cultures were grown in LB medium (1% w/w tryptone, 1% w/w NaCl, 0.5% w/w yeast extract) overnight at 30 °C. These were mixed in ratios of 1 part of the desired expression vector to 3 parts p19 vector (common suppressor of post-transcriptional gene silencing). This mixture was spun down, the supernatant removed, and the pellet was mixed with the activation buffer (200 mM MES at pH 5.6, 150 mM MgCl2, and 150 mM acetosyringone) and incubated at room temperature for at least 2 h to prime for the transformation. The Agrobacterium solution was infiltrated into the abaxial side of N. benthamiana leaves of 4-week-old plants, cultivated at 23 °C, 50% relative humidity and 12 h light/dark cycles. Protoplasts of leaf mesophyll tissue were obtained 3-5 days post infiltration.⁶⁰ One cm² squares of leaf tissue cut from transformed leaves were sliced in the lower epidermis and placed in 1 mL of 500 mM mannitol with the lower epidermis facing down for 1 h. The mannitol solution was then removed

and replaced by 500 μ L of protoplasting solution consisting of 10 mM CaCl₂, 5 mM MES, 50 mM mannitol, 3% cellulase, and 0.75% macerozyme, pH 5.6. The tissue was incubated at 26 °C on an orbital shaker at 100 rpm for 4 h. 0.5 volume of 200 mM CaCl₂ was then added, and the released protoplasts were pelleted by centrifugation. The protoplast pellet was resuspended in W5 solution consisting of 125 mM CaCl₂, 5 mM glucose, 5 mM KCl, and 1.5 mM NaCl, pH 5.6.

Zea Mays. The stable transformed line expressing pZmPIN1a::Zm-PIN1a-YFP in the inbred line B73 background was created by D. Jackson (Cold Spring Harbor Laboratory). 61 The yellow fluorescent protein YFP was inserted between the 218 and 219th amino acids of the PIN1a protein and stably expressed under its native PIN1a promoter. This line was cultured in a soil mix [0.16 m³ Metro-Mix 360 (Scotts, Marysville, OH, USA); 0.45 kg finely ground lime; 0.45 kg Peters Uni-Mix (JR Peters, Allentown, PA, USA); 68 kg Turface MVP (Profile Products, Buffalo Grove, IL, USA); 23 kg coarse quartz sand, and 0.018 m³ pasteurized field soil] at 16/8 h light/dark cycles. Protoplasts expressing pZmPIN1a::ZmPIN1a-YFP were isolated leaf tissue harvested after 2-4 weeks as described elsewhere. 62 The upper and lower 1/3 of the second youngest leaf was removed, and only the middle part was cut into 1 mm strips which were transferred to an enzyme solution (20 mL/0.5 g fresh weight tissue) consisting of 600 mM mannitol, 20 mM MES, pH 5.7, 20 mM KCl, 0.4% macerozyme R10 [Yakult Pharmaceuticals], 1.5% cellulase [Yakult Pharmaceuticals], 10 mM CaCl₂, and 0.1% BSA. The digestion was continued for 3 h in the dark under an 80 kPa vacuum. The protoplasts were filtered through a nylon mesh (100 μ M; Merck Millipore) and centrifuged for 1.5 min at 150g at 4 °C. The pellet was washed twice with 5 mL wash solution (600 mM mannitol, 4 mM MES, pH 5.7, and 20 mM KCl) and resuspended in MMG buffer (600 mM mannitol, 4 mM MES, pH 5.7, and 15 mM MgCl₂).

Validation of Protein Expression in Intact Plant Leaves and Protoplasts. Confocal imaging was performed using a Leica TCS SP5 or a Zeiss 710 confocal laser scanning microscope at excitation/emission wavelengths of 514/519–621 nm (for mCitrine and YFP), 488/493–698 nM for GFP, and 561/578–650 nm for mCherry to check the expression levels for the various stably and transiently expressed chimeras in the different plant species.

Formation of Vesicles from Plant Protoplasts. Protoplasts expressing a given chimera were pelleted at 250 rcf for 3 min, and cell bleb formation was induced by resuspending them in 4 mL of a blebbing buffer consisting of 500 mM Mannitol, 150 mM NaCl, 10 mM HEPES, 2 mM, $CaCl_2$, 25 mM formaldehyde (37% solution in water) (9 μ L/4 mL), 2 mM dithiothreitol (8 μ L/4 mL), pH 5.6, and incubating for 2 h at room temperature. The solution containing the protoplasts and blebbed vesicles was then centrifuged for 2 min at 200 rcf to pellet the protoplasts without rupturing them. The supernatant was collected, followed by another centrifugation of 5 min at 2000 rcf to clear cell debris from the supernatant. Membrane vesicles were collected from the top of the supernatant and stored at 4 °C in the dark before use. While the formaldehyde used in our blebbing buffer can have drawbacks at high concentrations, like cross-linking, the concentration used in the blebbing buffer is considerably less than that needed for fixing a cell. In mammalian systems, we have previously studied the effects of formaldehyde in the blebbing buffer and have concluded that we operate at a concentration with minimal impact on the protein's function. Other types of blebbing buffers can be used if this blebbing buffer is chemically incompatible with the system.⁶³

Plant Membrane Vesicle Labeling. Plant membrane vesicles were labeled with octadecyl rhodamine B chloride (R18, Molecular Probes), a lipophilic membrane dye that partitions into the bilayer and renders it fluorescent. R18 was added at a concentration of 4 μ L (0.36 mM) per 1 mL of plant vesicle solution and sonicated for 10 min. The excess free dye was then removed by size exclusion chromatography using a GE Healthcare Illustra MicroSpin G-25 Column at 250 rcf for 3 min. R18 fluorescence allowed the visualization of the supported membrane formation and confirmation of the 2D mobility of the resulting supported membrane by fluorescence recovery after photobleaching (FRAP), as described below.

Lipids and Liposome Preparation. Unilamellar liposomes were prepared via extrusion using the following synthetic lipids: 1-oleoyl-2palmitoyl-sn-glycero-3-phosphocholine (POPC) and 1-oleoyl-2-palmitoyl-sn-glycero-3-phosphocholine-polyethylene glycol (POPC-PEG-5000) (Avanti Polar Lipids). The liposomes were prepared by mixing the individual components in chloroform in a molar ratio of 99.5:0.5 in a 50 mL glass vial, prerinsed with ethanol and deionized water, and afterward dried for 30 min to remove residual water. The mixtures were combined from chloroform stock solutions, and the chloroform was gently evaporated using a stream of nitrogen, followed by a vacuum drying process under a deep vacuum for 3 h to remove residual chloroform. Liposomes were formed by adding GPMVM buffer to the dried lipid films to reach a concentration of 2 mg/mL concentration. Single unilamellar liposomes were subsequently prepared by extrusion through a 100 nm nanopore membrane (Whatman) with at least 10 passes using a Northern Lipids (Northbrook Court, Burnaby, BC, Canada) extruder. The liposomes were used without labeling.

Preparation and Formation of Planar Protoplast Supported Membranes. Microscope cover glass $(25 \times 25 \text{ mm}^2 \text{ No.1.5}, \text{ VWR})$ was used to create supported membranes. The surfaces were treated with a piranha solution [70% (v/v) H₂SO₄ (BDH) and 30% (v/v) H₂O₂ (Sigma 50 wt %)] for 10 min and rinsed with abundant amounts of deionized water. The polydimethylsiloxane (PDMS) wells holding the samples were made by mixing a 10:1 elastomer:cross-linker mixture of Sylgard 184 (Robert McKeown Company) and baked for 2 h at 80 °C. PDMS sheets were cut to fit over the coverslips completely and punched with a ~ 1 cm diameter hole, and the PDMS wells were affixed to the clean coverglass slides. 200 μL of labeled plant vesicle solution at approximately 8×10^6 vesicles/mL were added into the well and incubated for 20 min at room temperature. After incubation, the wells were rinsed gently with GPMV buffer (150 mM NaCl, 10 mM HEPES, 2 mM, CaCl₂, pH = 5.6) to remove all unattached vesicles. 50 μ L of liposome solution at a concentration of 2 mg/mL was added to the well and incubated for 30 min up to 3 h to form the supported plant membrane. After incubation, the sample was rinsed again with the GPMV buffer. Prior to supported membrane formation, the glass slides were scratched with a dissection tool and rinsed again with GPMV buffer to remove any released vesicles. The scratched-out area of the sample does not form a planar membrane and, therefore, allows the microscope to be focused at the right focal plane of the supported

Protoplast Vesicle Concentration, Size Distribution, and Charge. Nanoparticle tracking analysis (Nanosight NS300, Malvern) was used to determine the vesicle concentration and size distribution of the supernatant. Dynamic light scattering and electrophoretic light scattering (Zetasizer Nano ZS, Malvern) were used to measure the plant vesicles' size distribution and charge. All measurements were performed in GPMVM buffer (pH 5.6) at room temperature. All Light scattering and nanoparticle tracking measurements were performed in GPMVM buffer at pH 5.6 at room temperature as well. Five individual measurements, 60 s in duration, and 3 replicates were taken for each bleb type.

Transmission Electron Microscopy (TEM) of Blebs. Negative Stain TEM was used to determine the size and for microscopic examination of cellular blebs. The samples were imaged within 1 week of bleb production. To image the samples, 10 μ L of the bleb-containing buffer solution was deposited onto glow-discharged carbon-coated film 400 Mesh copper grids (Electron Microscopy Services, Hatfield, PA) and incubated for 5 min at room temperature. The grids were washed by first wicking away the sample solution using filter paper, then depositing 10 μ L of water and incubating for 2 min. The grid was subsequently stained with centrifuged 1% (v/v) uranyl acetate solution (Electron Microscopy Services, Hatfield, PA) and incubated for 2 min at room temperature. The uranyl acetate was wicked away, and the grid was dried prior to imaging. Talos F200C TEM was used for imaging at an accelerating voltage of 120 kV.

Verification of Supported Protoplast Membrane Formation by Fluorescence Microscopy. Formation of the protoplast membrane was visualized in real-time via fluorescence microscopy using an inverted Zeiss Axiovert Observer Z1 fluorescence microscope

 α Plan-Apochromat 40× objective, X-Cite 120 light source (Lumen Dynamics Group, Inc., Canada), coupled with a CCD camera (Hamamatsu ImageEM, model C9100-13, Bridgewater, NJ)]. Protoplast blebs were first labeled with R18 and incubated in a PDMS well, as described above. Vesicles adsorbed to the glass coverslip were observed as bright spots. When liposomes are added, they rupture on the glass and induce rupturing of neighboring plant vesicles, which can be observed as the R18 dye in the membranes of the vesicles diffuses in the plane of the newly formed planar bilayer (Supplemental Video 1). Supported membrane formation was further confirmed by FRAP and single protein tracking, as discussed in the following sections.

Fluorescence Recovery After Photobleaching. FRAP measurements were used to examine the diffusivity of the lipids within the protoplast membrane. The laser beam was used to bleach a $\sim 10~\mu m$ radius spot under a 40× objective, thereby photobleaching any R18 fluorophores within that zone. The fluorescence intensity was recorded for 15 min, as the bleached spot recovered with time. The fluorescence intensity of the spot was determined after background subtraction and normalization to minimize artifacts resulting from background photobleaching. The diffusivity (D) was calculated by fitting the recovery data to $D = w^2/4t_{1/2}$, where w is the full width at half-maximum of the Gaussian profile of the focused laser beam and $t_{1/2}$ is the characteristic diffusion time, as described by Soumpasis. 64 The fraction of fluorescence recovery provided a measure of the bilayer contiguity and completion of the rupture of the vesicles, as described in the main

Protein Orientation in the Supported Protoplast Membrane.

An enzymatic cleavage assay was used to characterize protein orientation in the membrane following standard protocols. Proteinase K (Ambion) was used to examine the orientation of mCitrine-RCI2A in the bilayer, as the conjugated fluorophore has a cleavage site (serine) for Proteinase K built into it between the label and the protein (Supplemental Figure 3). Protein expression was confirmed by imaging using a Total internal reflection fluorescence (TIRF) microscope (described next). Next, 100 μ L of Proteinase K at 100 μ g/mL was added on top of the protoplast-supported bilayer containing the protein. Images were acquired for an additional 10 min. If the cleavage site is accessible to the protease in the buffer, it will cleave off the fluorescent domain of the protein, allowing it to float out of the imaging range and resulting in a decrease in the fluorescence signal. On the contrary, if the protein is oriented the opposite way, the protease cannot access the cleavage site, and the fluorescence signal will not be lost.

Single-Molecule Tracking of Fluorescent Proteins in **Supported Protoplast Membranes.** Several single-particle tracking (SPT) methods have been reported in the literature. ^{28,65–67} Here, all the trajectories were found and calculated using the single-particle tracking method we previously published.⁶ Briefly, the location of the proteins was identified by their intensity, change of intensity from the previous frame, and displacement from the previous frame to find the match for every trajectory. ⁶⁸ Only trajectories that lasted for at least 20 frames (at the rate of 8 frames/s) were used to quantify the protein motion. Proteins that were confined to an area smaller than the maximum observed displacement for the fluorescent beads in the system were considered immobile.⁶⁷ The single-particle tracking algorithm uses the initial slope of the mean squared displacement (MSD) from the first three time-steps to determine the local homogeneous diffusion coefficient before confinement influences diffusion, thereby excluding the factor of bilayer heterogeneity and resultant changes in diffusion mode. 26,27,29 The moment scaling spectrum (MSS) analysis was used to access and quantify the bilayer heterogeneity and resultant changes in diffusion mode, objectively quantifying the mobility of a particle by a parameter denoted as β . ^{28,2} Here, β described the type of motion for each particle: β < 0.4 was confined diffusion; $0.4 \le \beta \le 0.6$ was quasi-free diffusion; $\beta > 0.6$ was convective diffusion. Total internal reflection microscopy (TIRF) was performed using an inverted Zeiss Axio Observer Z1 microscope with an α Plan-Apochromat 100× objective. The 488 nm wavelength from the solid-state lasers was used to excite the mCitrine-RCI2A and PIN1a-YFP within the membrane; the PIP2;1-mCherry within the membrane was exited with the 561 nm. A Laser TIRF 3 slider (Carl

Zeiss, Inc.) was used to control the angle of the incident beam. The excitation light was filtered by a Semrock LF488-B-ZHE filter cube and sent to an electron-multiplying CCD camera (ImageEM C9100-13, Hamamatsu). All the images were analyzed using Matlab (Mathworks) and ImageJ (NIH) with in-house scripts.6

Protein Subunit Counting. TIRF analysis of GFP quenching was performed as described previously using a custom-built azimuthal scanning objective-TIRF microscope based on an inverted microscope body (IX-81, Olympus) with a Flat-Top XYZ automated stage (Applied Scientific Instrumentation).⁶⁹ Single-molecule imaging was performed on the GFP-tagged AtFLOT1 and 2, exciting it using a 488 nm laser (Spectra-Physics) directed to the sample through an acoustic-opticaltunable filter (AA Optoelectronics) to enable precise excitation intensity modulation. The detection pathway consisted of a TuCam adapter (Andor Technologies) equipped with a band-pass filter (ET525/41) to isolate and direct the GFP signal onto an EMCCD (iXon 887, Andor Technologies). Stepwise photobleaching data were analyzed using a custom lab software package (ImageC.exe, written in C/C++ under Microsoft Visual Studio 2017), which identified fluorescent puncta and recorded the intensity vs time trace. Briefly, ImageC.exe automatically locates fluorescent puncta above a threshold that meets a specified Gaussian fit criterion by successive processing of the summed image stack. For each molecule, a region of interest (ROI) (typically 5×5) centered on the pixel containing the centroid was created, and the ROI mean values vs time (frame) were extracted from the stack. Traces without discernible bleach steps were discarded. The data are presented without subtracting the background fluorescence.

ASSOCIATED CONTENT

Supporting Information

The Supporting Information is available free of charge at https://pubs.acs.org/doi/10.1021/acsami.3c18562.

Bleb characteristics, fluorescence recovery data of A. thaliana SLB and Z. mays SLB, protein sequence of RCI2A-mCitrine and cleavage sites, scrambled orientation experiment, single protein tracking analysis of PIN1a-YFP in Z. mays, RCI2A-mCitrine in A. thaliana, and PIN1-GFP in A. thaliana supported bilayers (PDF)

Rupturing, the formation of planar bilayer patches, and the healing together of the patch edges as the process proceeds (MP4)

Rupture, bilayer formation, and subsequent protein diffusion in 2D are readily apparent (AVI)

A fully formed bilayer with PIP2;1-mCherry diffusing and colored trajectories of the protein pathways superimposed on the images with each time step (AVI)

AUTHOR INFORMATION

Corresponding Author

Susan Daniel – RF Smith School of Chemical and Biomolecular Engineering, Cornell University, Ithaca, New York 14853, *United States;* orcid.org/0000-0001-7773-0835; Email: sd386@cornell.edu

Authors

Martin Stuebler – RF Smith School of Chemical and Biomolecular Engineering, Cornell University, Ithaca, New York 14853, United States; University of Natural Resources and Life Sciences, Vienna 1180, Austria

Zachary A. Manzer - RF Smith School of Chemical and Biomolecular Engineering, Cornell University, Ithaca, New York 14853, United States; o orcid.org/0000-0002-8225-8990

- Han-Yuan Liu RF Smith School of Chemical and Biomolecular Engineering, Cornell University, Ithaca, New York 14853, United States
- Julia Miller School of Integrative Plant Science, Cornell University, Ithaca, New York 14853, United States
- Annett Richter Boyce Thompson Institute, Ithaca, New York 14853, United States
- Srinivasan Krishnan Boyce Thompson Institute, Ithaca, New York 14853, United States
- Ekaterina Selivanovitch RF Smith School of Chemical and Biomolecular Engineering, Cornell University, Ithaca, New York 14853, United States
- Barituziga Banuna RF Smith School of Chemical and Biomolecular Engineering, Cornell University, Ithaca, New York 14853, United States
- Georg Jander Boyce Thompson Institute, Ithaca, New York 14853, United States; oorcid.org/0000-0002-9675-934X
- Erik Reimhult University of Natural Resources and Life Sciences, Vienna 1180, Austria; oorcid.org/0000-0003-1417-5576
- Warren R. Zipfel Meinig School of Biomedical Engineering, Cornell University, Ithaca, New York 14853, United States
- Adrienne H. K. Roeder School of Integrative Plant Science, Cornell University, Ithaca, New York 14853, United States; Weill Institute for Cell and Molecular Biology, Cornell University, Ithaca, New York 14853, United States; orcid.org/0000-0001-6685-2984
- Miguel A. Piñeros School of Integrative Plant Science, Cornell University, Ithaca, New York 14853, United States; Robert W. Holley Center for Agriculture & Health, ARS-USDA, Ithaca, New York 14853, United States

Complete contact information is available at: https://pubs.acs.org/10.1021/acsami.3c18562

Author Contributions

^OM.S. and Z.A.M. contributed equally to this work.

Notes

The authors declare no competing financial interest.

ACKNOWLEDGMENTS

We thank Josh Strable and Mike Scanlon for providing pZmPIN1a::ZmPIN1a-YFP kernels and access to a growth chamber with conditions optimized for Z. mays growth. We thank Maria Harrison at the Boyce Thompson Institute for providing the PIP2;1-mCherry construct. We thank Michal Daněk for the 35S::AtFLOT1-GFP and 35S::AtFLOT2-GFP constructs. H.-Y.L. and Z.A.M. acknowledge funding from the Fleming Fellowship at the RF Smith School of Chemical and Biomolecular Engineering at Cornell University. Z.A.M. acknowledges support from the Cornell CBI Training Program funded by the National Institute of Health/National Institute of General Medical Sciences grant T32GM138826. A.R. was funded by a fellowship from the Deutsche Forschungsgemeinschaft. G.J. acknowledges the Binational Agricultural Research and Development Fund, award US-4846-15C. A.H.K.R. acknowledges funding from the NSF IOS 1553030. S.D. acknowledges funding from the National Science Foundation 2016107.

REFERENCES

(1) Martiniére, A.; Lavagi, I.; Nageswaran, G.; Rolfe, D. J.; Maneta-Peyret, L.; Luu, D.-T.; Botchway, S. W.; Webb, S. E. D.; Mongrand, S.;

- Maurel, C.; Martin-Fernandez, M. L.; Kleine-Vehn, J.; Friml, J.; Moreau, P.; Runions, J. Cell Wall Constrains Lateral Diffusion of Plant Plasma-Membrane Proteins. *Proc. Natl. Acad. Sci. U. S. A.* **2012**, *109*, 12805—12810.
- (2) Siontorou, C. G.; Nikoleli, G.-P.; Nikolelis, D. P.; Karapetis, S. K. Artificial Lipid Membranes: Past, Present, and Future. *Membranes* **2017**, *7* (3), 38.
- (3) Chan, Y.-H. M.; Boxer, S. G. Model Membrane Systems and Their Applications. *Curr. Opin. Chem. Biol.* **2007**, *11* (6), 581–587.
- (4) Pace, H.; Simonsson Nyström, L.; Gunnarsson, A.; Eck, E.; Monson, C.; Geschwindner, S.; Snijder, A.; Hook, F. Preserved Transmembrane Protein Mobility in Polymer-Supported Lipid Bilayers Derived from Cell Membranes. *Anal. Chem.* **2015**, 87 (18), 9194–9203.
- (5) Svetlova, A.; Ellieroth, J.; Milos, F.; Maybeck, V.; Offenhäusser, A. Composite Lipid Bilayers from Cell Membrane Extracts and Artificial Mixes as a Cell Culture Platform. *Langmuir* **2019**, *35* (24), 8076–8084.
- (6) Richards, M. J.; Hsia, C.-Y.; Singh, R. R.; Haider, H.; Kumpf, J.; Kawate, T.; Daniel, S. Membrane Protein Mobility and Orientation Preserved in Supported Bilayers Created Directly from Cell Plasma Membrane Blebs. *Langmuir* **2016**, *32* (12), 2963–2974.
- (7) Liu, H.-Y.; Grant, H.; Hsu, H.-L.; Sorkin, R.; Bošković, F.; Wuite, G.; Daniel, S. Supported Planar Mammalian Membranes as Models of in Vivo Cell Surface Architectures. *ACS Appl. Mater. Interfaces* **2017**, 9 (41), 35526–35538.
- (8) Kiessling, V.; Domanska, M. K.; Murray, D.; Wan, C.; Tamm, L. K. Supported Lipid Bilayers. In *Wiley encyclopedia of chemical biology*; Wiley, 2007; pp. 112.
- (9) Castellana, E. T.; Cremer, P. S. Solid Supported Lipid Bilayers: From Biophysical Studies to Sensor Design. *Surf. Sci. Rep.* **2006**, *61* (10), 429–444.
- (10) Cordelier, S.; Crouzet, J.; Gilliard, G.; Dorey, S.; Deleu, M.; Dhondt-Cordelier, S. Deciphering the Role of Plant Plasma Membrane Lipids in Response to Invasion Patterns: How Could Biology and Biophysics Help? *J. Exp. Bot.* **2022**, 73 (9), 2765–2784.
- (11) Furlan, A. L.; Laurin, Y.; Botcazon, C.; Rodríguez-Moraga, N.; Rippa, S.; Deleu, M.; Lins, L.; Sarazin, C.; Buchoux, S. Contributions and Limitations of Biophysical Approaches to Study of the Interactions between Amphiphilic Molecules and the Plant Plasma Membrane. *Plants* 2020, 9 (5), 648.
- (12) Sivankalyani, V.; Geetha, M.; Subramanyam, K.; Girija, S. Ectopic Expression of Arabidopsisrci2a Gene Contributes to Cold Tolerance in Tomato. *Transgenic Res.* **2015**, *24*, 237–251.
- (13) Da Ines, O.; Graf, W. P.; Franck, K. I.; Albert, A.; Winkler, J. B.; Scherb, H.; Stichler, W.; Schäffner, A. R. Kinetic Analyses of Plant Water Relocation Using Deuterium as Tracer Reduced Water Flux of Arabidopsis Pip2 Aquaporin Knockout Mutants. *Plant Biol.* **2010**, *12* (Suppl 1), 129–139.
- (14) Verdoucq, L.; Grondin, A.; Maurel, C. Structure-Function Analysis of Plant Aquaporin Atpip2;1 Gating by Divalent Cations and Protons. *Biochem. J.* **2008**, 415 (3), 409–416.
- (15) Thompson, M. V.; Wolniak, S. M. A Plasma Membrane-Anchored Fluorescent Protein Fusion Illuminates Sieve Element Plasma Membranes in Arabidopsis and Tobacco. *Plant Physiol.* **2008**, *146* (4), 1599–1610.
- (16) Okada, K.; Ueda, J.; Komaki, M. K.; Bell, C. J.; Shimura, Y. Requirement of the Auxin Polar Transport System in Early Stages of Arabidopsis Floral Bud Formation. *Plant Cell* **1991**, 3 (7), 677–684.
- (17) Liu, H.-Y.; Chen, W.-L.; Ober, C. K.; Daniel, S. Biologically Complex Planar Cell Plasma Membranes Supported on Polyelectrolyte Cushions Enhance Transmembrane Protein Mobility and Retain Native Orientation. *Langmuir* **2018**, *34* (3), 1061–1072.
- (18) Mohamed, Z.; Shin, J.-H.; Ghosh, S.; Sharma, A. K.; Pinnock, F.; Bint E Naser Farnush, S.; Dorr, T.; Daniel, S. Clinically Relevant Bacterial Outer Membrane Models for Antibiotic Screening Applications. ACS Infect. Dis. 2021, 7 (9), 2707–2722.
- (19) Kaufmann, S.; Papastavrou, G.; Kumar, K.; Textor, M.; Reimhult, E. A Detailed Investigation of the Formation Kinetics and Layer

- Structure of Poly (Ethylene Glycol) Tether Supported Lipid Bilayers. *Soft Matter.* **2009**, *5* (14), 2804–2814.
- (20) Dugas, C. M.; Li, Q.; Khan, I. A.; Nothnagel, E. A. Lateral Diffusion in the Plasma Membrane of Maize Protoplasts with Implications for Cell Culture. *Planta* **1989**, *179* (3), 387–396.
- (21) Roeder, A. H.; Chickarmane, V.; Cunha, A.; Obara, B.; Manjunath, B.; Meyerowitz, E. M. Variability in the Control of Cell Division Underlies Sepal Epidermal Patterning in Arabidopsis Thaliana. *PloS Biol.* **2010**, *8* (5), No. e1000367.
- (22) Albertorio, F.; Diaz, A. J.; Yang, T.; Chapa, V. A.; Kataoka, S.; Castellana, E. T.; Cremer, P. S. Fluid and Air-Stable Lipopolymer Membranes for Biosensor Applications. *Langmuir* **2005**, *21* (16), 7476–7482.
- (23) De Gennes, P. G. Scaling Concepts in Polymer Physics; Cornell University Press: Ithaca, N.Y, 1979.
- (24) Marsh, D.; Bartucci, R.; Sportelli, L. Lipid Membranes with Grafted Polymers: Physicochemical Aspects. *Biochim. Biophys. Acta. Biomembr.* **2003**, *1615* (1), 33–59.
- (25) Renner, L.; Pompe, T.; Lemaitre, R.; Drechsel, D.; Werner, C. Controlled Enhancement of Transmembrane Enzyme Activity in Polymer Cushioned Supported Bilayer Membranes. *Soft Matter.* **2010**, 6 (21), 5382–5389.
- (26) Kusumi, A.; Sako, Y.; Yamamoto, M. Confined Lateral Diffusion of Membrane Receptors as Studied by Single Particle Tracking (Nanovid Microscopy). Effects of Calcium-Induced Differentiation in Cultured Epithelial Cells. *Biophys. J.* **1993**, *65* (5), 2021–2040.
- (27) Smith, P. R.; Morrison, I. E.; Wilson, K. M.; Fernandez, N.; Cherry, R. J. Anomalous Diffusion of Major Histocompatibility Complex Class I Molecules on Hela Cells Determined by Single Particle Tracking. *Biophys. J.* **1999**, *76* (6), 3331–3344.
- (28) Ferrari, R.; Manfroi, A.; Young, W. Strongly and Weakly Self-Similar Diffusion. *Physica D: Nonlinear Phenomena* **2001**, 154 (1–2), 111–137.
- (29) Sbalzarini, I. F.; Koumoutsakos, P. Feature Point Tracking and Trajectory Analysis for Video Imaging in Cell Biology. *J. Struct. Biol.* **2005**, *151* (2), 182–195.
- (30) Li, X.; Wang, X.; Yang, Y.; Li, R.; He, Q.; Fang, X.; Luu, D.-T.; Maurel, C.; Lin, J. Single-Molecule Analysis of Pip2; 1 Dynamics and Partitioning Reveals Multiple Modes of Arabidopsis Plasma Membrane Aquaporin Regulation. *Plant Cell* **2011**, 23 (10), 3780–3797.
- (31) Hosy, E.; Martiniére, A.; Choquet, D.; Maurel, C.; Luu, D.-T. Super-Resolved and Dynamic Imaging of Membrane Proteins in Plant Cells Reveal Contrasting Kinetic Profiles and Multiple Confinement Mechanisms. *Mol. Plant* **2015**, 8 (2), 339–342.
- (32) Martiniére, A.; Fiche, J. B.; Smokvarska, M.; Mari, S.; Alcon, C.; Dumont, X.; Hematy, K.; Jaillais, Y.; Nollmann, M.; Maurel, C. Osmotic Stress Activates Two Reactive Oxygen Species Pathways with Distinct Effects on Protein Nanodomains and Diffusion. *Plant Physiol.* **2019**, *179* (4), 1581–1593.
- (33) Saffman, P. G.; Delbrück, M. Brownian Motion in Biological Membranes. *Proc. Natl. Acad. Sci. U. S. A.* 1975, 72 (8), 3111–3113.
- (34) Martiniére, A.; Runions, J. Protein Diffusion in Plant Cell Plasma Membranes: The Cell-Wall Corral. *Front. Plant Sci.* **2013**, *4*, 515.
- (35) Kleine-Vehn, J.; Wabnik, K.; Martiniére, A.; Łangowski, Ł.; Willig, K.; Naramoto, S.; Leitner, J.; Tanaka, H.; Jakobs, S.; Robert, S.; Luschnig, C.; Govaerts, W.; W Hell, S.; Runions, J.; Friml, J. Recycling, Clustering, and Endocytosis Jointly Maintain Pin Auxin Carrier Polarity at the Plasma Membrane. *Mol. Syst. Biol.* **2011**, *7* (1), 540.
- (36) Feraru, E.; Feraru, M. I.; Kleine-Vehn, J.; Martiniére, A.; Mouille, G.; Vanneste, S.; Vernhettes, S.; Runions, J.; Friml, J. Pin Polarity Maintenance by the Cell Wall in Arabidopsis. *Curr. Biol.* **2011**, *21* (4), 338–343.
- (37) Daněk, M.; Valentová, O.; Martinec, J. Flotillins Erlins, and Hirs: From Animal Base Camp to Plant New Horizons. *Crit. Rev. Plant Sci.* **2016**, 35 (4), 191–214.
- (38) Hao, H.; Fan, L.; Chen, T.; Li, R.; Li, X.; He, Q.; Botella, M. A.; Lin, J. Clathrin and Membrane Microdomains Cooperatively Regulate Rbohd Dynamics and Activity in Arabidopsis. *Plant Cell* **2014**, *26* (4), 1729–1745.

- (39) Jarsch, I. K.; Konrad, S. S. A.; Stratil, T. F.; Urbanus, S. L.; Szymanski, W.; Braun, P.; Braun, K.-H.; Ott, T. Plasma Membranes Are Subcompartmentalized into a Plethora of Coexisting and Diverse Microdomains in Arabidopsis and Nicotiana Benthamiana. *Plant Cell* **2014**, *26* (4), 1698–1711.
- (40) Li, R.; Liu, P.; Wan, Y.; Chen, T.; Wang, Q.; Mettbach, U.; Baluška, F.; Šamaj, J.; Fang, X.; Lucas, W. J.; Lin, J. A Membrane Microdomain-Associated Protein, Arabidopsis Flot1, Is Involved in a Clathrin-Independent Endocytic Pathway and Is Required for Seedling Development. *Plant Cell* **2012**, 24 (5), 2105–2122.
- (41) Borner, G. H. H.; Sherrier, D. J.; Weimar, T.; Michaelson, L. V.; Hawkins, N. D.; MacAskill, A.; Napier, J. A.; Beale, M. H.; Lilley, K. S.; Dupree, P. Analysis of Detergent-Resistant Membranes in Arabidopsis. Evidence for Plasma Membrane Lipid Rafts. *Plant Physiol.* **2005**, *137* (1), 104–116.
- (42) Daněk, M.; Angelini, J.; Malínská, K.; Andrejch, J.; Amlerová, Z.; Kocourková, D.; Brouzdová, J.; Valentová, O.; Martinec, J.; Petrášek, J. Cell Wall Contributes to the Stability of Plasma Membrane Nanodomain Organization of Arabidopsis Thaliana Flotillin2 and Hypersensitive Induced Reaction1 Proteins. *Plant J.* **2020**, *101* (3), 619–636.
- (43) Wang, P.; Dong, Y.; Zhu, L.; Hao, Z.; Hu, L.; Hu, X.; Wang, G.; Cheng, T.; Shi, J.; Chen, J. The Role of Gamma-Aminobutyric Acid in Aluminum Stress Tolerance in a Woody Plant, Liriodendron Chinense X Tulipifera. *Hortic. Res.* **2021**, *8* (1), 80.
- (44) Solis, G. P.; Hoegg, M.; Munderloh, C.; Schrock, Y.; Malaga-Trillo, E.; Rivera-Milla, E.; Stuermer, C. A. O. Reggie/Flotillin Proteins Are Organized into Stable Tetramers in Membrane Microdomains. *Biochem. J.* **2007**, 403 (2), 313–322.
- (45) Ulbrich, M. H.; Isacoff, E. Y. Subunit Counting in Membrane-Bound Proteins. *Nat. Methods* **2007**, *4* (4), 319–321.
- (46) McKenna, J. F.; Rolfe, D. J.; Webb, S. E. D.; Tolmie, A. F.; Botchway, S. W.; Martin-Fernandez, M. L.; Hawes, C.; Runions, J. The Cell Wall Regulates Dynamics and Size of Plasma-Membrane Nanodomains in I Arabidopsis I. *Proc. Natl. Acad. Sci. U. S. A.* **2019**, *116* (26), 12857–12862.
- (47) Chadda, R.; Bernhardt, N.; Kelley, E. G.; Teixeira, S. C. M.; Griffith, K.; Gil-Ley, A.; Öztürk, T. N.; Hughes, L. E.; Forsythe, A.; Krishnamani, V.; Faraldo-Gómez, J. D.; Robertson, J. L. Membrane Transporter Dimerization Driven by Differential Lipid Solvation Energetics of Dissociated and Associated States. *eLife* **2021**, *10*, No. e63288.
- (48) Charalambous, K.; Miller, D.; Curnow, P.; Booth, P. J. Lipid Bilayer Composition Influences Small Multidrug Transporters. *BMC Biochem.* **2008**, *9* (1), 31.
- (49) Stieger, B.; Steiger, J.; Locher, K. P. Membrane Lipids and Transporter Function. *Biochim. Et Biophys. Acta Mol. Basis Dis.* **2021**, 1867 (5), 166079.
- (50) Helenius, A.; Simons, K. A. I. Solubilization of Membranes by Detergents. *Biochimica Et Biophy. Acta Rev. Biomembr.* **1975**, 415 (1), 29–79.
- (51) Rajendran, L.; Simons, K. Lipid Rafts and Membrane Dynamics. *J. Cell Sci.* **2005**, *118* (6), 1099–1102.
- (52) Lee, A. G. How Lipids Affect the Activities of Integral Membrane Proteins. *Biochim. Biophys. Acta Biomembr.* **2004**, *1666* (1–2), 62–87.
- (53) Monnier, N.; Furlan, A. L.; Buchoux, S.; Deleu, M.; Dauchez, M.; Rippa, S.; Sarazin, C. Exploring the Dual Interaction of Natural Rhamnolipids with Plant and Fungal Biomimetic Plasma Membranes through Biophysical Studies. *Int. J. Mol. Sci.* **2019**, *20* (5), 1009.
- (54) Zhang, Y.; Wustoni, S.; Savva, A.; Giovannitti, A.; McCulloch, I.; Inal, S. Lipid Bilayer Formation on Organic Electronic Materials. *J. Mater. Chem. C* **2018**, *6* (19), 5218–5227.
- (55) Pappa, A. M.; Liu, H. Y.; Traberg-Christensen, W.; Thiburce, Q.; Savva, A.; Pavia, A.; Salleo, A.; Daniel, S.; Owens, R. M. Optical and Electronic Ion Channel Monitoring from Native Human Membranes. *ACS Nano* **2020**, *14* (10), 12538–12545.
- (56) Pantoja, O. Recent Advances in the Physiology of Ion Channels in Plants. *Annu. Rev. Plant Biol.* **2021**, 72 (1), 463–495.

- (57) Benková, E.; Michniewicz, M.; Sauer, M.; Teichmann, T.; Seifertová, D.; Jürgens, G.; Friml, J. Local Efflux-Dependent Auxin Gradients as a Common Module for Plant Organ Formation. *Cell* **2003**, 115 (5), 591–602.
- (58) Birnbaum, K.; Jung, J. W.; Wang, J. Y.; Lambert, G. M.; Hirst, J. A.; Galbraith, D. W.; Benfey, P. N. Cell Type—Specific Expression Profiling in Plants Via Cell Sorting of Protoplasts from Fluorescent Reporter Lines. *Nat. Methods* **2005**, *2* (8), 615–619.
- (59) Ivanov, S.; Harrison, M. J. A Set of Fluorescent Protein-Based Markers Expressed from Constitutive and Arbuscular Mycorrhiza-Inducible Promoters to Label Organelles, Membranes and Cytoskeletal Elements in Medicago Truncatula. *Plant J.* **2014**, *80* (6), 1151–1163.
- (60) Waadt, R.; Kudla, J. In Planta Visualization of Protein Interactions Using Bimolecular Fluorescence Complementation (Bifc). CSH Protoc. 2008, 2008 (4), pdb-prot4995.
- (61) Gallavotti, A.; Yang, Y.; Schmidt, R. J.; Jackson, D. The Relationship between Auxin Transport and Maize Branching. *Plant Physiol.* **2008**, *147* (4), 1913–1923.
- (62) Richter, A.; Schaff, C.; Zhang, Z.; Lipka, A. E.; Tian, F.; Köllner, T. G.; Schnee, C.; Preiß, S.; Irmisch, S.; Jander, G.; Boland, W.; Gershenzon, J.; Buckler, E. S.; Degenhardt, J. Characterization of Biosynthetic Pathways for the Production of the Volatile Homoterpenes Dmnt and Tmtt in Zea Mays. *Plant Cell* **2016**, 28 (10), 2651–2665.
- (63) Sezgin, E.; Kaiser, H.-J.; Baumgart, T.; Schwille, P.; Simons, K.; Levental, I. Elucidating Membrane Structure and Protein Behavior Using Giant Plasma Membrane Vesicles. *Nat. Protoc.* **2012**, *7* (6), 1042–1051.
- (64) Soumpasis, D. Theoretical Analysis of Fluorescence Photobleaching Recovery Experiments. *Biophys. J.* **1983**, *41* (1), 95–97.
- (65) Vrljic, M.; Nishimura, S. Y.; Moerner, W. Single-Molecule Tracking. In *Lipid Rafts*; Springer, 2007. pp. 193219.
- (66) Sonnleitner, A.; Schütz, G.; Schmidt, T. Free Brownian Motion of Individual Lipid Molecules in Biomembranes. *Biophys. J.* **1999**, 77 (5), 2638–2642.
- (67) Poudel, K. R.; Jones, J. P.; Brozik, J. A. A Guide to Tracking Single Transmembrane Proteins in Supported Lipid Bilayers. In *Lipid-Protein Interactions*; Springer, 2013. pp. 233252.
- (68) Smith, M. B.; Karatekin, E.; Gohlke, A.; Mizuno, H.; Watanabe, N.; Vavylonis, D. Interactive, Computer-Assisted Tracking of Speckle Trajectories in Fluorescence Microscopy: Application to Actin Polymerization and Membrane Fusion. *Biophys. J.* **2011**, *101* (7), 1794–1804.
- (69) Manzer, Z. A.; Ghosh, S.; Jacobs, M. L.; Krishnan, S.; Zipfel, W. R.; Piñeros, M.; Kamat, N. P.; Daniel, S. Cell-Free Synthesis of a Transmembrane Mechanosensitive Channel Protein into a Hybrid-Supported Lipid Bilayer. *ACS Appl. Bio. Mater.* **2021**, *4* (4), 3101–3112.
- (70) Singh, A.; Van Slyke, A. L.; Sirenko, M.; Song, A.; Kammermeier, P. J.; Zipfel, W. R. Stoichiometric Analysis of Protein Complexes by Cell Fusion and Single Molecule Imaging. *Sci. Rep.* **2020**, *10* (1), 14866.